D2.2: R&D report on Laboratory developments of the best recycling methods to produce high-quality recyclates from EOL composite materials for the GO/NO-GO decision

WP2

NTUA

Funded by
the European Union

TECHNICAL REFERENCES

Grant Agreement Number	101096437
Project Acronym	BLADES2BUILD
Project Title	Recycle, Repurpose and Reuse end-of-life wind blade composites – A coupled pre- and co-processing demonstration
Funding Scheme	HORIZON-CL5-2022-D3-01-02
Project Coordinator	Ana Teresa Macas Lima Technical University of Denmark atmli@dtu.dk
Project Website	www.blades2build.com
Project Duration	January 2023 – December 2025 (36 months)

Deliverable No.	D2.2: R&D report on Laboratory developments of the best recycling methods to produce high-quality recyclates from EOL composite materials for the GO/NO-GO decision
Type / Dissemination level[1]	R — Document, report
Work Package	WP2 - Testing and Identification of Scalable Circularity Frameworks
Task	T2.2 - Improvement of Recycling technologies to have Higher Quality Recycled Materials
Lead beneficiary	NTUA
Contributing beneficiary/ies	DTU
Due date of deliverable	31 12 2024
Actual submission date	07 01 2025
Status	Final

Version	Date	Beneficiary	Author
V0.1	01/12/2024	NTUA	Maria MODESTOU
V0.2	06/12/2024	DTU	Tao LIU

[1]PU – Public, fully open, e.g., web (Deliverables flagged as public will be automatically published in CORDIS project's page)
SEN – Sensitive, limited under the conditions of the Grant Agreement
Classified R-UE/EU-R – EU RESTRICTED under the Commission Decision No2015/444
Classified C-UE/EU-C – EU CONFIDENTIAL under the Commission Decision No2015/444
Classified S-UE/EU-S – EU SECRET under the Commission Decision No2015/444

AUTHORING AND APPROVALS

Prepared		
Name	Organization	Position and title
Maria MODESTOU	NTUA	R&D Engineer
Spyros SOULIS	NTUA	R&D Engineer
Tao LIU	DTU	Postdoc researcher

Reviewed			
Name	Organization	Position	Date
	DTU	Coordinator	
	ACCIONA		
	HIC		
	LM WIND		
Dionisis SEMITEKOLOS Costas CHARITIDIS	NTUA	Project Manager Lab Director	04/12/20241
	TU/e		
	RWTH AACHEN		
	RENAO		
	CESPA		
	ENDESA		
	PZE		
	GE WIND		
	GCS		
	ELDAN		

Approved			
Name	Organization	Position	Date

DISCLAIMER AND PROPRIETARY RIGHTS STATEMENT

This project has received funding from the European Union's Horizon Europe research and innovation programme under the grant agreement No. 101096437.

Funded by the European Union. Views and opinions expressed are however those of the author(s) only and do not necessarily reflect those of the European Union or the European Climate, Infrastructure and Environment Executive Agency (CINEA). Neither the European Union nor the granting authority can be held responsible for them.

TABLE OF CONTENTS

LIST OF TABLES

LIST OF FIGURES

LIST OF ABBREVIATIONS

CA – Consortium Agreement

D – Deliverable

T – Task

M – Month

PM – Person Month

DoA – Description of Action

DoW – Description of Work

EC – European Commission

FP – Framework Programme

GA – General Agreement

PO – Project officer

PC – Project Coordinator

PP – Programme Participants

PU – Public

PTC – Project Technical Committee

SME – Small and Medium Enterprises

LE – Large Enterprises

TM – Technical Manager

IPR – Intellectual Property Right

PC – Project Coordinator

SC – Steering Committee

SME – Small and Medium Enterprise

WP – Work package

WTB – Wind Turbine Blades

1 EXECUTIVE SUMMARY

Blades2Build project, under WP2, aimed to evaluate and optimize various recycling methods for WTB waste, addressing challenges associated with the end-of-life management of these composite materials. The focus was placed on exploring thermal, chemical, and mechanical recycling techniques, with the goal of developing processes that maximize material recovery, minimize environmental impact, and ensure industrial scalability.

Chemical recycling was explored through low-temperature solvolysis using a Poly(ethylene glycol)/NaOH system and supercritical solvolysis with acetone. These methods focused on breaking down the polymer matrix to recover clean fibres while evaluating the effects of catalysts and solvents on fibre quality and process efficiency. The study compared the operational conditions, such as temperatures and pressures, and analysed fibre properties using advanced characterization techniques like SEM and EDX.

The thermal recycling approach involved a two-step thermolysis process, comprising pyrolysis in a nitrogen atmosphere and oxidation or sintering in air. This method was investigated to recover the inorganic components, primarily glass fibres, from WTB waste. The study optimized process parameters, including heating cycles and batch sizes, and explored techniques such as sieving and flotation to improve the quality of the final product. Additionally, thermogravimetric analysis (TGA) provided insights into the thermal degradation behaviour of GFRP materials under different atmospheric conditions.

Mechanical recycling, conducted by DTU and PreZero, investigated the shredding and sieving of WTB waste into different particle-sized fractions. This approach was evaluated for its potential to produce materials suitable for use as fillers or reinforcements in construction applications. The particle size distribution and its influence on cement mortar were analysed to assess the suitability of this method for downstream applications.

This deliverable presents the methodologies, experimental setups, and results for all three recycling methods, offering a detailed account of the processes developed and optimized during the project. The findings provide a solid foundation for advancing circular economy principles in the wind energy sector and contribute to reducing the environmental impact of WTB waste.

Keywords: WTB recycling, pyrolysis, chemical solvolysis, supercritical acetone, mechanical recycling, glass fibre recovery, sustainability, circular economy.

2 METHODOLOGY

2.1 WTB Waste Identification & Characterisation

The raw material used consisted of fractions of varying sizes, presumably obtained through the sieving of shredded initial waste. Although the material was primarily composed of glass fibre-reinforced polymer (GFRP), it was inherently an inhomogeneous mixture, containing other materials such as wood fragments and various residuals. This variability presented unique challenges in processing and recovering high-quality recyclates. Due to the lack of datasheets or relevant information regarding the waste materials, it was necessary to conduct an analysis of the composition of the WTB wastes. Fourier-transform infrared (FT-IR) spectroscopy was employed to identify the chemical composition of the resin matrix and other impurities. This method provided insights into the functional groups present in the polymeric matrix, helping to distinguish between different resin types. FT-IR spectroscopy was conducted using a Cary 630 spectrometer (Agilent), which operates within a wavelength range of 4000–400 cm^{-1} and has a resolution of 4 cm^{-1}. Ten randomly selected composite waste samples and 8 different impurities were analysed to determine their composition, for the material identification.

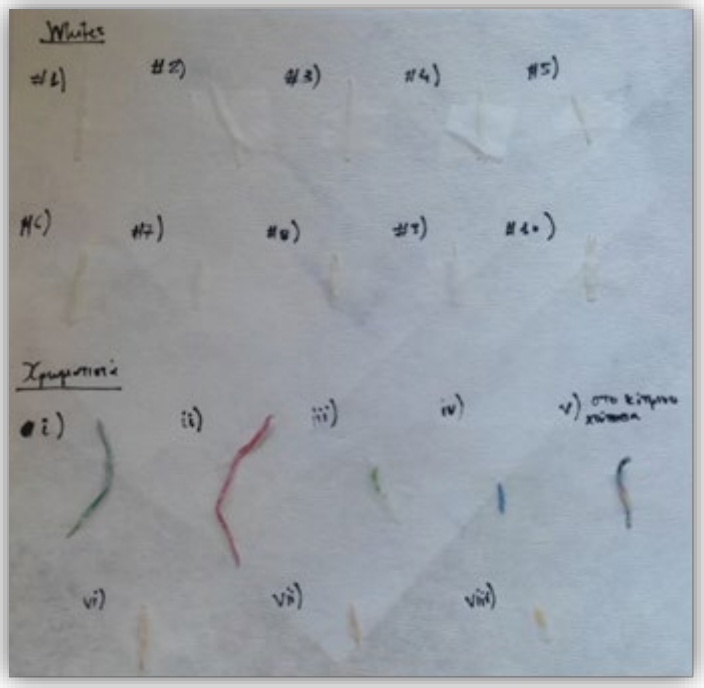

Figure 1: Ten different composite samples and eight different impurities from initial waste.

2.2 Chemical Recycling

Chemical recycling involves the chemical breakdown of the polymer matrix and the recovery of fibres from composite materials. The primary methods explored include solvolysis at low temperatures and ambient pressure, as well as solvolysis under near- or supercritical conditions (Morin, Loppinet-Serani, Cansell, & Aymonier, 2012; Oliveux, Bailleul, & Salle, 2012). Solvolysis uses a variety of solvents such as water, alcohols, acetone, glycol, or acids to recover and reuse the fibres (Podara, Termine, & Modestou, 2024). The flexibility of solvolysis lies in its wide range of solvent choices, catalysts, and processing conditions (temperature and pressure) to break down the polymer matrix of materials such as epoxy, polyester, or phenolic resins.

Low-temperature solvolysis is typically performed below 200°C and at atmospheric pressure, where the use of acids and catalysts is necessary to effectively degrade the resin under mild conditions. In contrast, sub- and supercritical solvolysis is a newer, more eco-friendly, and sustainable process, though it requires advanced, costly equipment due to the need for high-pressure systems instead of relying on catalysts or toxic solvents (Morici & Dintcheva, 2022). Sub- and supercritical fluids such as water, acetone, and alcohol are highly effective reaction media for the depolymerization or decomposition of thermoplastics and thermosets, and they can be recovered and reused, further enhancing the sustainability of the process (Podara, Termine, & Modestou, 2024).

This research specifically targets the recycling of WTB through a two-case low-temperature solvolysis using Formic Acid and a poly(ethylene glycol)/NaOH system (Dang, Kubouchi, Sembokuya, & Tsuda, 2005), as well as supercritical solvolysis with acetone. enhancing the process's sustainability. This particular research targets the recycling of WTBs through low-temperature solvolysis using a poly(ethylene glycol)/NaOH system, as well as supercritical solvolysis with acetone.

2.2.1 Low temperature and pressure Solvolysis

The recycling process using formic acid at its boiling point was tested with various ratios of composite waste mass to solvent volume over a 4-hour period. However, it was found that large quantities of formic acid were necessary to achieve satisfactory results, resulting in excessive liquid waste and high solvent requirements. Due to these inefficiencies, the method was deemed unsuitable, and no further research was pursued.

In the Poly(ethylene glycol)/NaOH system, polymer degradation occurs through glycolysis, driven by nucleophilic substitution reactions between the reagents. NaOH introduces hydroxyl anions, which are attracted to the electrophilic centres of the ester bonds within the polymer chains. This process effectively breaks the ester bonds, decomposing the polyester matrix into smaller oligomers and monomers. The experiments were carried out in a 500 ml three-necked round-bottom flask

equipped with a reflux condenser and magnetic stirring, at 200°C with different parameters being adjusted, such as the reaction time and the mass of NaOH.

Figure 2: Experimental Setup

Table 1. Experimental Parameters and Conditions.

Exp.	Amount of PEG200 (g)	Amount of NaOH (g)	Amount of WTB wastes (g)	Reaction Time (hours)	Stirring Speed (rpm)
1	200	1	10	4	200
2	200	3	10	4	200
3	200	3	10	5.5	200
4	200	8	10	4	200
5	200	8	10	5.5	200
6	200	10	10	4	200
7	200	10	10	5.5	200
8	200	10	5	4	200
9	200	20	10	5.5	200
10	200	20	10	4	200
11	200	15	10	5.5	200
12	200	15	10	4	200
13	200	12.5	10	5.5	200
14	200	12.5	10	4	200

The process was further scaled up in a 2-liter reactor equipped with mechanical stirring. During this scale-up, it was observed that a reduced amount of NaOH was needed to achieve similar results. This reduction was attributed to the improved mixing efficiency provided by mechanical stirring, which offers greater torque and is especially advantageous for reactions involving high viscosity or complexity, where enhanced mixing power improves the overall process. Subsequently, the process was scaled up again in a 10-liter batch reactor, also equipped with mechanical stirring. In this setup, 333g of composite material were added to 5 litres of PEG200 and heated at the same temperature (200°C) used in the laboratory-scale reactor for 5.5 hours under atmospheric pressure.

Figure 3: 10-litre Batch Reactor

Due to the slower heating rate in the 10-liter reactor, NaOH was introduced at three distinct elevated temperatures (80°C, 120°C, and 170°C) to allow for better control of the reaction. Adding NaOH progressively, rather than all at once at the start, helped manage the reaction kinetics more effectively and prevented the risk of thermal runaway.

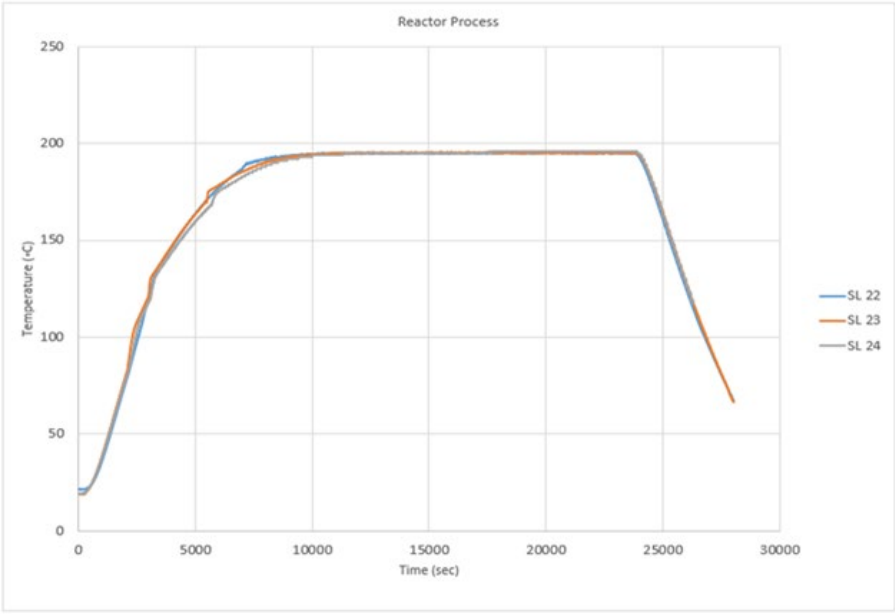

Figure 4: Reactor Temperature Profile

Process temperature profile was also investigated to ensure stability and repeatability of the solvolysis reaction. The successful validation of the temperature profile and the effective control of

the reaction kinetics allowed for further optimization of critical process parameters. This optimization resulted in a reduction in the overall reaction time to 5 hours, while the stirring speed was decreased to 100 rpm, maintaining efficient mixing throughout the reaction. Under these optimized conditions, a series of 15 experiments was conducted. Through this process, approximately 2.7 kg of glass fibres were successfully recovered, meeting the material needs of the project partners for subsequent research and development activities.

2.2.2 Solvolysis at near- or supercritical conditions

The mechanism of solvolysis with supercritical acetone, a polar aprotic solvent, is based on nucleophilic substitution (SN_2) reactions. The oxygen of the carbonyl group in acetone attacks the electrophilic carbon atoms of the ester bonds in unsaturated polyester, resulting in the cleavage of bonds and the formation of oligomers and monomers.

For the supercritical solvolysis process, a 4-litre autoclave reactor, filled with 2 litres of acetone and equipped with mechanical stirring at 200 rpm, was used. The system operated under supercritical temperatures and pressures, with key parameters such as temperature, reaction time, and WTB waste mass being adjusted to determine the optimal conditions for matrix degradation and fibre recovery.

Figure 5: Autoclave Reactor

Table 2. Experimental Parameters and Conditions

Exp.	Amount of WTB wastes (g)	Reaction Time (hours)	Reaction Temperature (°C)	Reaction Pressure (bar)
1	150	1	240	50
2	100	2	250	67
3	100	2	300	144
4	100	2	350	195
5	100	3	300	141
6	100	3	325	174
7	100	2	325	174
8	100	3.5	350	216
9	100	4	350	218
10	100	3	350	213
11	100	2.5	350	210
12	125	4	350	222
13	150	4	350	224
14	175	4	350	222
15	200	4	350	222

2.3 Thermal Recycling

Thermal recycling involves the thermal decomposition of the polymer matrix through high-temperature processes, enabling the recovery of fibres and other materials from composite waste. The thermal recycling of WTB waste focused on the recovery of the glass fibres, through the controlled decomposition of the matrix material. An initial thermolysis trial was conducted using 20 g of mixed-sized scrap, where non-GFRP pieces were manually removed, along with a relatively large piece of WTB scrap measuring approximately 15 cm in length. Leveraging prior expertise in processing carbon fibre-reinforced polymer (CFRP) composites, a batch process consisting of two sequential steps was employed: pyrolysis in an inert nitrogen atmosphere, followed by high-temperature oxidation in an air atmosphere.

2.3.1 Lab Scale Thermolysis

Figure 6 shows the treatment parameters and the results of each step on the large GFRP sample. During Step 1 (pyrolysis), the GFRP piece was transformed into a black material, commonly referred to as char, which retained its structural coherence to a significant degree. However, in Step 2 (oxidation), the material fully disintegrated, leaving behind glass fibres. Initial trials confirmed that the char produced during pyrolysis exhibited flame resistance at room temperature, validating its carbonaceous nature.

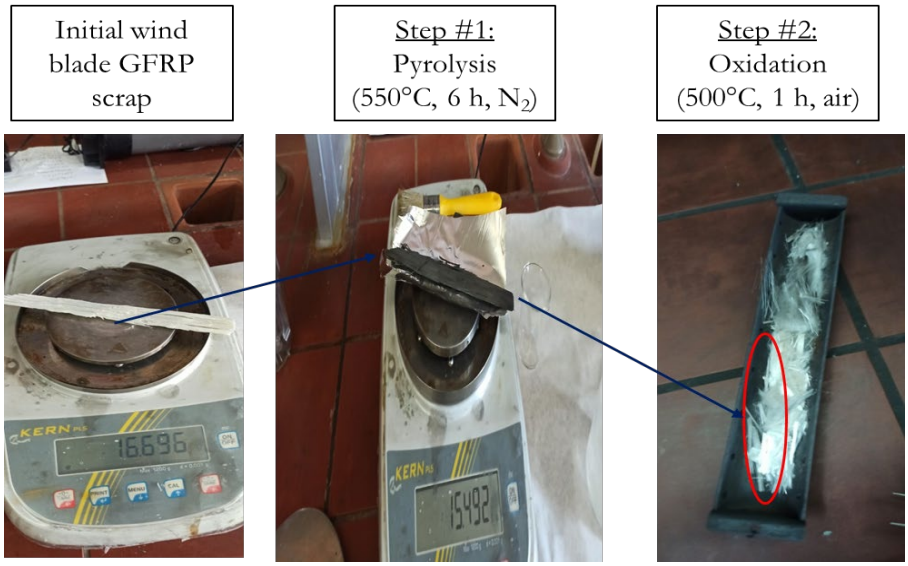

Figure 6: First trial with two-step GFRP thermolysis - effect of treatments on the product.

Following the initial trial and incorporating insights from the TGA measurements, thermolysis was conducted in a tubular oven as a batch process consisting of two sequential stages: pyrolysis and oxidation. During the pyrolysis stage, the polymer matrix was decomposed in an inert nitrogen atmosphere. The process began with dynamic heating of the WTB waste sample up to 550°C over a period of 70 minutes, followed by isothermal conditioning at 550°C for 360 minutes under nitrogen flow.

After completing the pyrolysis, the nitrogen flow was stopped, and the material was exposed to an oxidative air atmosphere at the same temperature of 550°C for an additional 60 minutes, continuing until cooldown. This controlled two-step process ensured effective decomposition of the matrix during pyrolysis and complete removal of residual char during oxidation, leaving behind clean glass fibres suitable for recovery.

2.3.2 Upscaling and Refinement

Throughout the project, the thermolysis process was progressively upscaled and refined to improve efficiency. Initial runs began with a GFRP waste feed of 60 g, which was gradually increased to 100–

150 g and eventually scaled up to 300 g per batch. Concurrently, the initial heating program, which lasted over 8 hours, was optimized into a shorter but higher-temperature heating cycle of approximately 1.5 hours.
During the thermolysis process, particularly in the pyrolysis stage, significant amounts of gases and tarry byproducts were observed. The evolution of gases began at approximately 300°C, while tarry byproducts appeared around 430°C. As the process was scaled up, managing these exhaust gases became increasingly challenging, necessitating the installation of a specialized collector system with a cooling trap, as shown in Figure 7.

Figure 7: Cooling trap setup used for cleaning the gaseous byproducts of the thermolysis.

Over 3.5 kg of thermolysis product had been produced across 33 batch runs. The experimental plan systematically investigated different process parameters, yielding several key findings. Table 3 summarizes the conditions and the yield for all the runs performed.

Regarding particle size, the initial trial (Run #1) indicated that particle size had no significant effect on yield. However, from Runs #2 to #18, a particle size of 1–2 mm was preferred for better packing in the sample holder. After transitioning to a perforated cylinder sample holder, larger particle sizes of 14–20 mm were used from Runs #19 to #27. For Runs #21 and #22, hand-selected GFRP waste resulted in a notably higher yield, underscoring the potential of pre-sorting the feed material. After Run #28, technical limitations required a return to the smaller, boat-type holder and particle sizes of 1–2 mm.

Table 3: Thermolysis experiments of WTB waste.

Run #	Mass of sample (g)	THERMOLYSIS PROGRAM				Products (g)		Efficiency (%)	Notes
		STEP #1 Pyrolysis		STEP #2 Oxidation		Main	Side		
		Temperature (°C)	Time (min)	Temperature (°C)	Time (min)				
1	70	550	300	550	60	44.5		72.9	Multi-fraction feed
2	90	550	96	550	25	43.7	70.2	64.9	From here on: Single fraction feed (1-2 mm)- large volume of gaseous and tarry byproducts
3	110	550	91	550	54	51.1	78.4	60.8	Installing collector (i.e. cooling trap) for gaseous byproduct processing
4	120	550	90	550	57	58.9	77.3	61.3	Improving the collector
5	130	550	86	550	55	55.5	80.0	60.0	Further improving the collector
6	125	550	85	550	60	54.8	80.6	59.7	Blasting hot air during oxidation
7	130	550	65	550	60	34.8	79.1	60.5	Low product quality
8	125	550	61	550	85	38.4	80.3	59.8	Low product quality
9	125	500	87	500	56	81.75		69.2	Incomplete oxidation / Very low product quality
10	125	550	100	550	50	77.9		75.4	Low product quality
11	130	555	85	555	65	77.5		80.8	Medium product quality
12	135	555	90	555	60	81.3		79.6	Medium product quality
13	110	555	90	555	60	66.1		79.8	Medium product quality

14	255	550	170	600	60	143.2	87.7	Pyrolysis with separate sintering
15	257.9	550	170	600	60	140.0	91.4	Pyrolysis with separate sintering
16	225.0	550	110	600	60	140.0	75.6	Pyrolysis with separate sintering
17	245.2	550	170	600	60	140.5	85.4	Pyrolysis with separate sintering
18	258.3	550	170	600	100	139.2	92.2	Pyrolysis with separate sintering
19	270	550	90	600	100	163.2	79.1	Change of sample holder -> change of particle size fraction (14-20 mm) / Pyrolysis with separate sintering
20	241.4	550	90	600	100	130.2	92.1	Particle size fraction (14-20 mm) / Pyrolysis with separate sintering
21	150.0	RT - 760	90 (ramp)	760-RT	60 (ramp)	97.7	69.7	Particle size fraction (14-20 mm) / Pyrolysis with separate sintering
22	237.3	RT - 760	90 (ramp)	760-RT	60 (ramp)	151.8	72.1	Particle size fraction (14-20 mm) / Pyrolysis with separate sintering
23	250.0	RT - 850	90 (ramp)	850-RT	60 (ramp)	136.6	90.7	Particle size fraction (14-20 mm) / Pyrolysis with separate sintering
24	270.0	RT - 760	90 (ramp)	760-RT	60 (ramp)	142.9	94.1	Particle size fraction (14-20 mm) / Pyrolysis with separate sintering / Medium quality product
25	290.0	RT - 760	90 (ramp)	760-RT	60 (ramp)	171.3	81.9	Particle size fraction (14-20 mm) / Pyrolysis with separate sintering
26	300.0	RT - 760	90 (ramp)	760-RT	60 (ramp)	159.4	93.7	Particle size fraction (14-20 mm) / Pyrolysis with separate sintering

27	300.0	RT - 760	90 (ramp)	760-RT	60 (ramp)	164.4	90.4	Particle size fraction (14-20 mm) / Pyrolysis with separate sintering
28	180.0	RT - 760	90 (ramp)	760-RT	60 (ramp)	97.3	91.9	Particle size fraction (1-2 mm) / Pyrolysis with separate sintering
29	170.0	RT - 760	90 (ramp)	760-RT	60 (ramp)	95.1	88.1	Particle size fraction (1-2 mm) / Pyrolysis with separate sintering
30	180.0	RT - 760	90 (ramp)	760-RT	60 (ramp)	94.9	94.6	Particle size fraction (1-2 mm) / Pyrolysis with separate sintering
31	180.0	RT - 760	90 (ramp)	760-RT	60 (ramp)	98.3	90.8	Particle size fraction (1-2 mm) / Pyrolysis with separate sintering
32	180.0	RT - 760	90 (ramp)	760-RT	60 (ramp)	98.0	91.1	Particle size fraction (1-2 mm) / Pyrolysis with separate sintering
33	180.0	RT - 760	90 (ramp)	760-RT	60 (ramp)	110.7 (Therm) 52.0	77.0	Particle size fraction (1-2 mm) / Split in two parts after thermolysis for sieving / Sintered mass 60.2 g

The heating program was also optimized. In Run #2, it was determined that a pyrolysis duration of 90 minutes achieved results comparable to those of a 6-hour treatment, while between Runs #14 and #18, increasing residence time during pyrolysis showed no impact on product quality. A faster temperature ramping program up to 760°C was tested in Run #21 and yielded results identical to those achieved at 550°C for 90 minutes. To address issues with carbon residuals on the material at the ends of the boat-type holder, additional sintering at 600°C for 30–50 minutes was implemented after Run #14. As batch sizes exceeded 200 g, oxidation in the oven proved inefficient, leading to the replacement of the oxidation step with sintering at 600°C after Run #20. Attempts to improve oxidation efficiency, such as blasting hot air into the oven (Run #6), did not yield significant benefits.

Despite variations in particle size, batch size, and treatment conditions, the overall yield of the thermolysis process showed little fluctuation. The mean thermolysis yield was 55.0% (standard deviation 1.9%), reflecting the proportion of inorganic residuals in the initial waste. The pyrolysis yield averaged 64.5% (standard deviation 2.0%), while the apparent yield from the oxidation or sintering step was 86.9% (standard deviation 2.5%). Notably, runs #21 and #22, which utilized a more GFRP-rich feed, resulted in higher thermolysis yields of 64.5% (standard deviation 0.8%) and pyrolysis yields of 72.1% (standard deviation 2.2%). These findings highlight the potential for improved process efficiency through pre-sorting of the feed material, such as using flotation to separate GFRP particles from the WTB waste.

2.4 Mechanical Recycling

Mechanical recycling involves the physical processing of composite waste to recover and repurpose the waste as fibres reinforcement materials in new applications. The mechanical recycling of WTB waste focuses on the size reduction and reconditioning of GFRP for use in mortar as reinforcement.

The WTB was subjected to a mechanical process of shredding. The initial size reduction was performed using a high-torque shredder, breaking down the WTB scrap into manageable pieces with lengths ranging from 5μm–10 cm.

The recovered GFRP were sieved to ensure uniform size distribution, removing fines and oversized fragments. The resulting wind turbine blade fibres (WTBF) were incorporated into mortar mixes to partially replace conventional reinforcement, optimizing workability and strength properties. This approach leverages the intrinsic mechanical properties of the recovered fibres, contributing to the sustainability and circular economy of construction materials.

After shredding, the recovered GFRP was sieved to determine its particle size distribution. The raw material and mass fraction of WTBF after the sieving process are presented in Figure 8. The red dashed line shows the incremental WTBF waste (shown in Figure 8 (b)). The incremental waste percentage remains relatively low and stable for particle sizes below 1000 μm. However, a noticeable increase occurs beyond this threshold, with a sharp peak at larger particle sizes, indicating a significant proportion of the WTBF is found in these coarser fractions. The solid black line represents the cumulative WTBF waste, which shows a progressive accumulation of WTBF waste as the particle size increases. The cumulative WTBF remains steady up to approximately 100 μm but then rises more rapidly. A sharp incline occurs after 1000 μm, reflecting the substantial contribution of larger particles to the total WTBF waste. This trend reaches its maximum as the cumulative WTBF approaches 100%, confirming that the majority of the WTBF is concentrated in larger particle sizes. Figure 9 shows the WTBF from mechanical recycling in the mortar as fibre reinforcement.

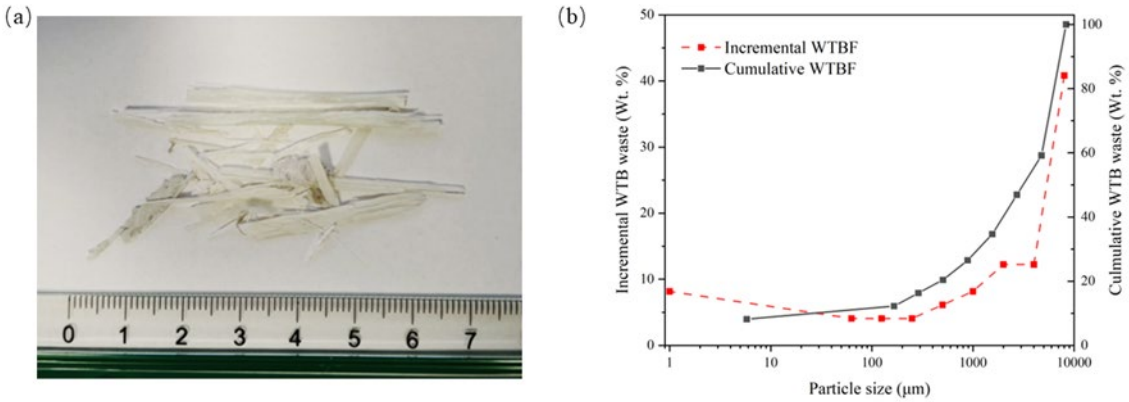

Figure 8: Raw WTBF before sieving; (b) Particle size distribution of WTBF after sieving test.

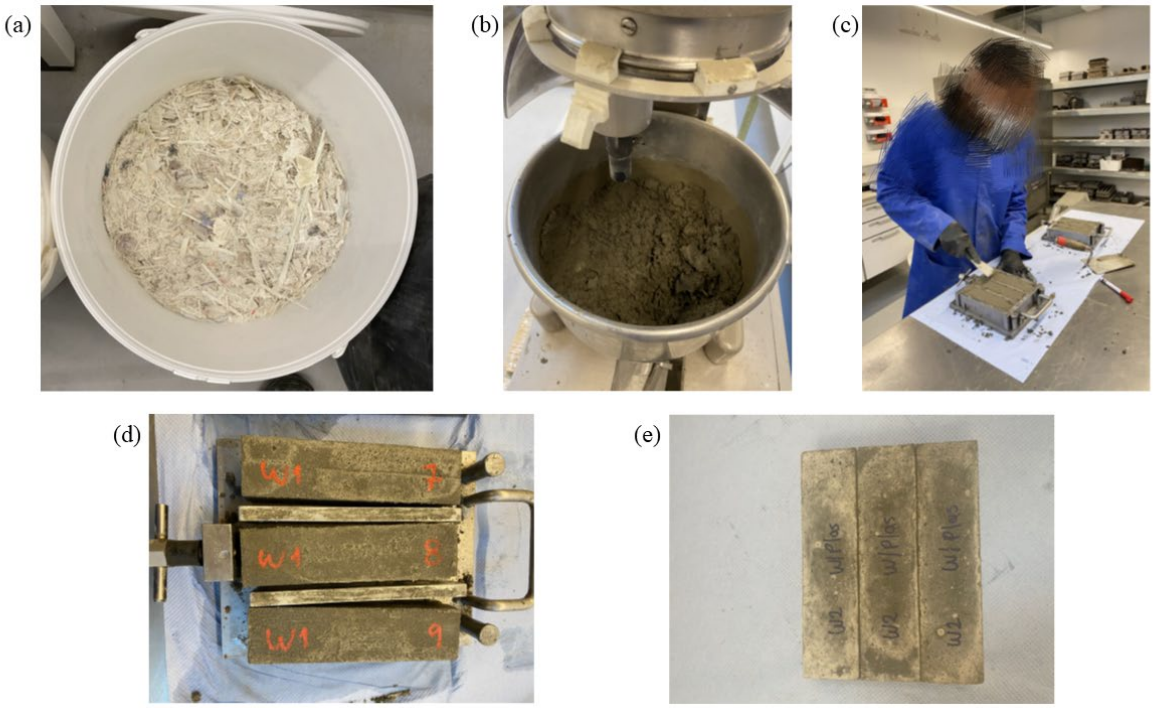

Figure 9: (a) WTBF used in mortar; (b) Mixing process; (c) Molding process; (d) Demolding process; (e) Mortar prisms.

3 RESULTS

3.1 WTB Waste Identification & Characterisation

3.1.1 Composite Waste

Ten spectra were obtained from ten different waste particles. No sample preparation was performed, resulting in inhomogeneity among the samples regarding both thickness and surface area. In Figure 10 the spectra of the ten white samples display characteristic peaks associated with unsaturated polyester (Koto & Soegijono, 2019), (Chukwu, Madueke, & Ekebafe, 2019). Variations in transmittance intensities and slight shifts in the peaks are observed due to sample non-uniformity and the possible presence of impurities.

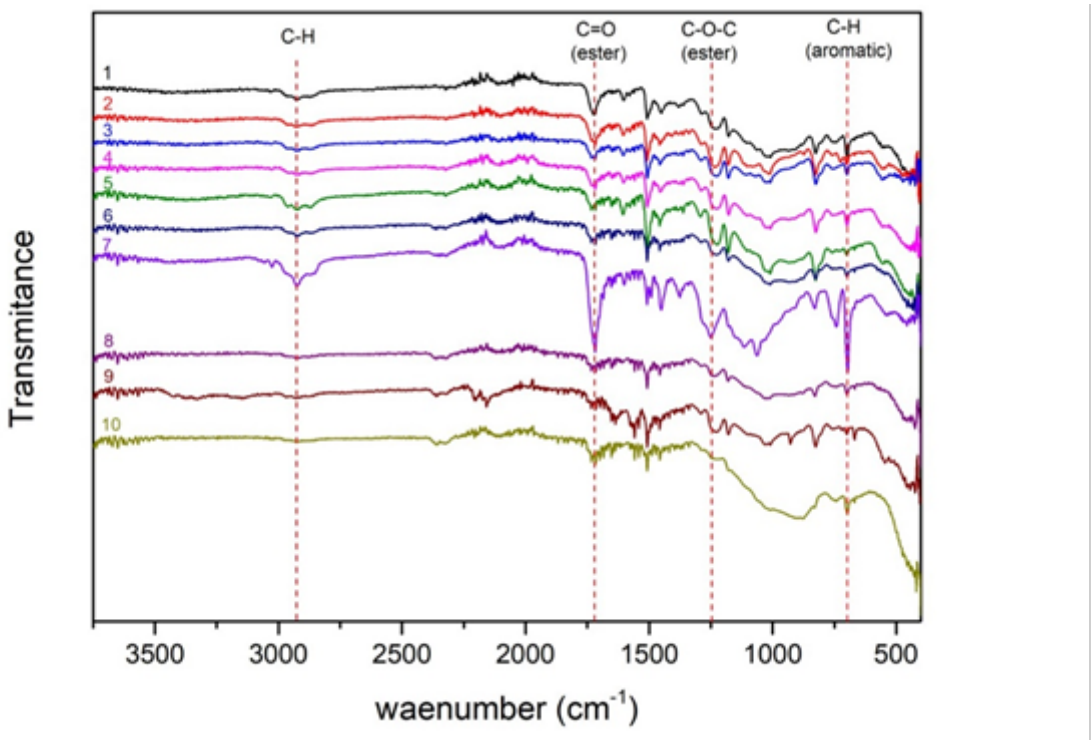

Figure 10: FT-IR Spectra of 10 different composite wastes.

Figure 9 shows the representative spectrum of glass reinforced polymer particle, which is the main phase of the WTB waste. The prominent peak at 1730 cm^{-1} indicates that the matrix of the GFRP is unsaturated polyester (UP). This was further confirmed by the presence of two peaks at 982 and 912 cm^{-1} (as the inset in Figure 9 shows), which can be attributed to the unreacted double bonds originating from maleate and styrene units, respectively. The presence of unreacted bonds in the UP is not a surprise, given that double bonds in cured UP do not react completely - even after protracted post curing (Simitzis, 2002).

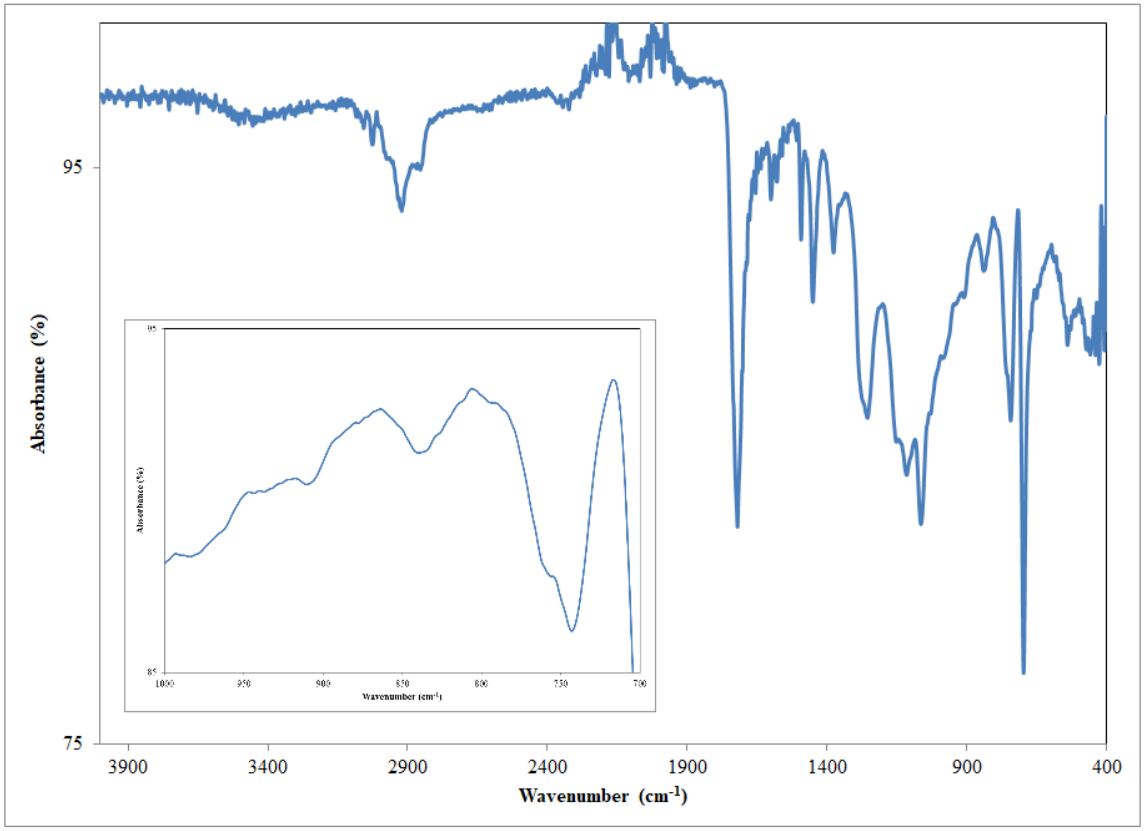

Figure 9. FTIR spectrum of GFRP waste

3.1.2 Impurities

Eight different impurities were selected from the initial waste.

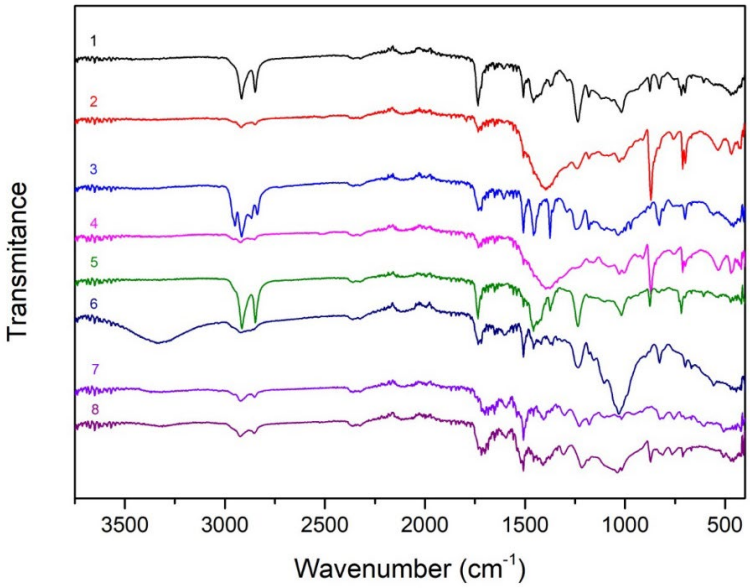

Figure 11: FT-IR Spectra of 8 different impurities in the initial waste mixture.

We can distinguish five different materials in the above spectra (Figure 11). Spectra 1 and 5, 2 and 4, as well as 7 and 8, are found to be identical.

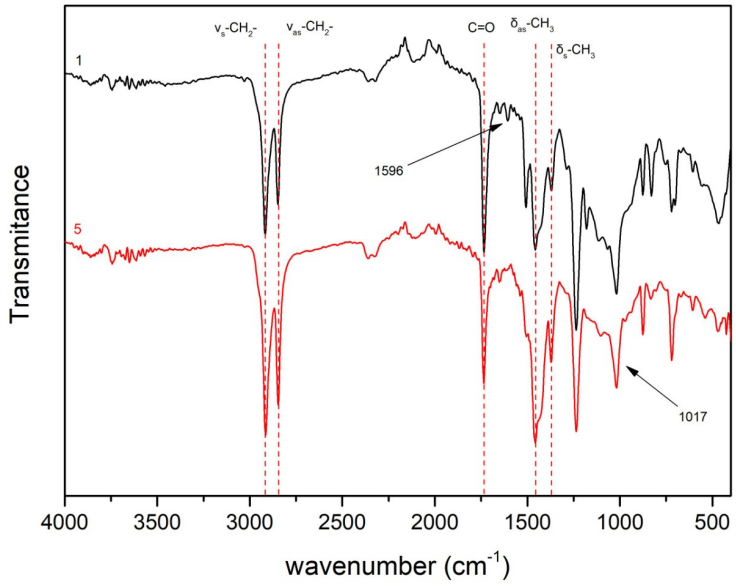

Figure 12: FT-IR Spectrums of 1 & 5.

The samples corresponding to spectra 1 and 5, as depicted in the Figure, consist of thin films of a thermoplastic polymer. The presence of pigments influences the spectra, but the material appears to be a mixture of PP/PE or possibly COC (cyclic olefin copolymer), given the appearance of peaks at 1596 cm^{-1} and 1017 cm^{-1} (Gopanna, Mandapati, & Thomas, 2019). Furthermore, the peak observed at 1733 cm^{-1} corresponds to C=O and is characteristic of waste polyolefins, suggesting oxidation due to degradation (Nafchi, Abdouss, Najafi, Gargari, & Mazhar, 2015).

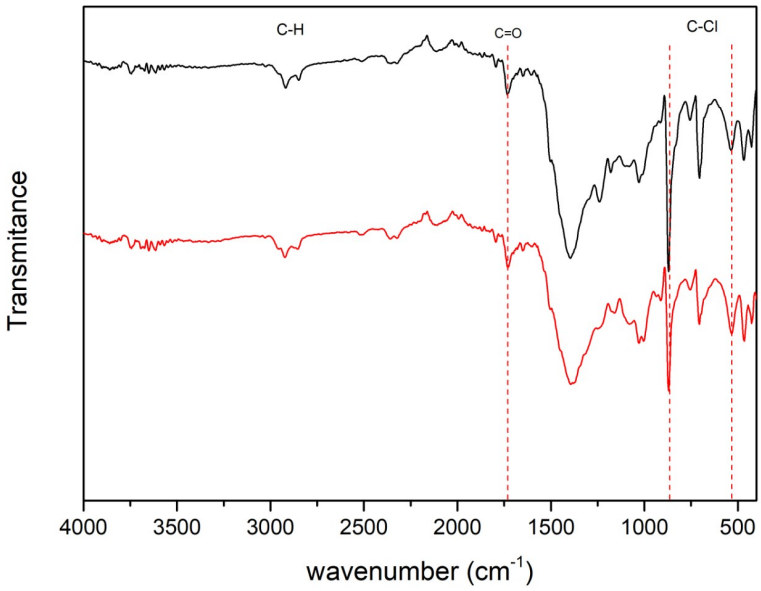

Figure 13: FT-IR Spectrums of 2 & 4.

Spectra 2 and 4 are likely associated with PVC, as they exhibit a characteristic peak of the C-Cl vibration at 844 cm^{-1} (Ul-Hamid, Al-Soufi, Al-Hadhrami, & Shemsi, 2015), (Pandey, Joshi, Mukherjee, & Thomas, 2016). Additionally, the peak at 1729 cm^{-1} indicates oxidation corresponding to C=O, which is still observable in these spectra.

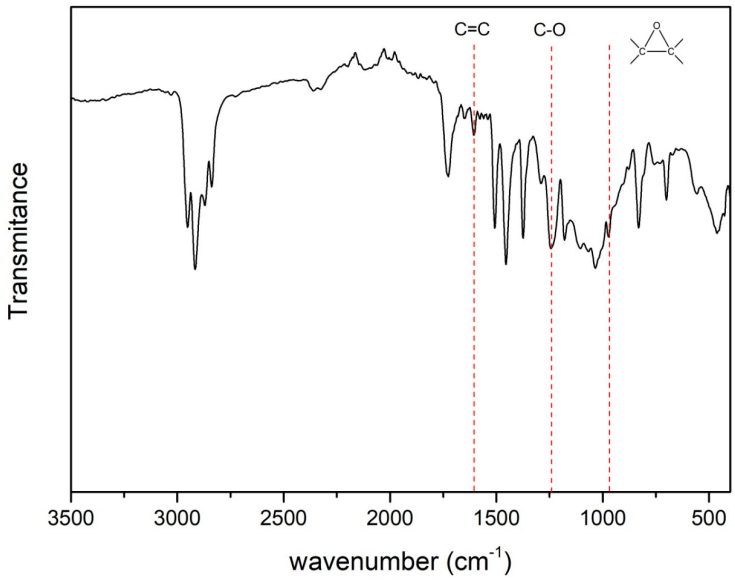

Figure 14: FT-IR Spectrum of 3.

Sample 3 is likely composed of epoxy resin or a mixture of epoxy and phenolic materials (Fernandes, et al., 2018), (Zhang & Liu, 2020). The presence of several peaks is also influenced by the dye (green) used in the sample. Considering the information from Vestas' material passport, it is known that WTB waste contains epoxy gel coats, which could be the source of this sample.

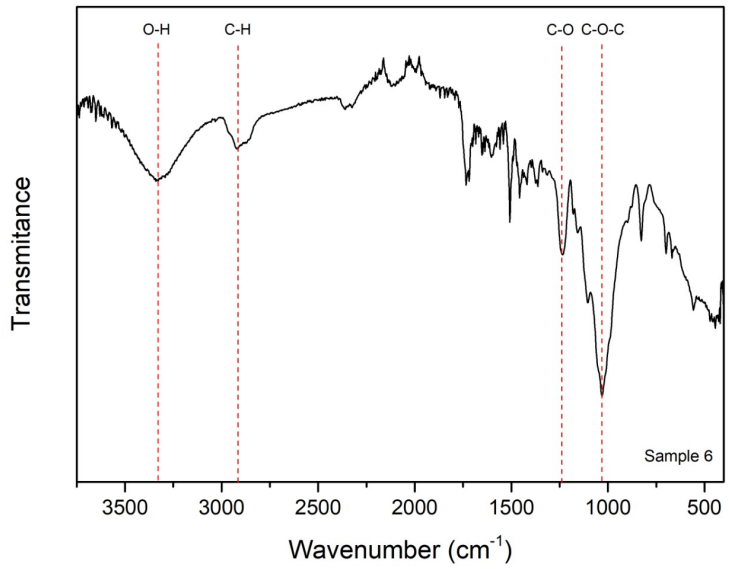

Figure 15: FT-IR Spectrum of 6.

Spectrum 6 shows the characteristic peaks of wood (Emmanuel, Odile, & Céline, 2015).

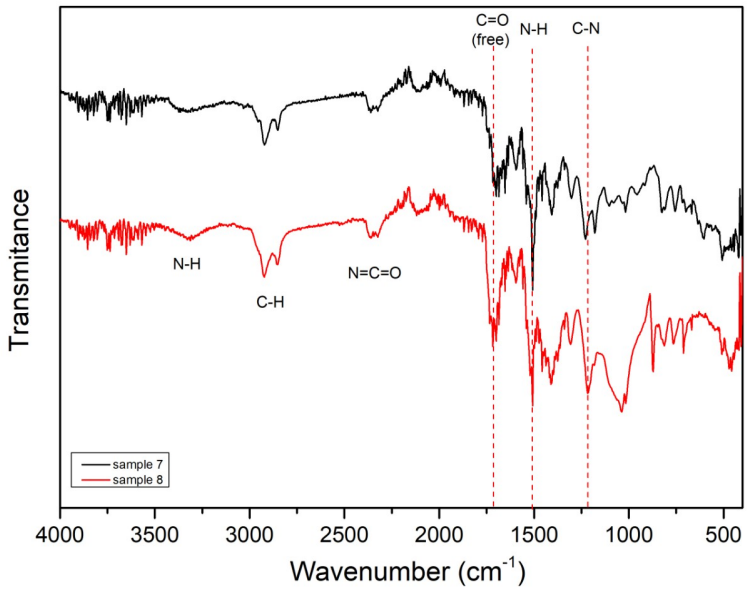

Figure 16: FT-IR Spectrums of 7 & 8.

The spectra of samples 7 and 8 exhibit poor quality and significant noise. Despite the limitations, the observable peaks suggest that the material is likely PU (polyurethane) (Kosmela, Hejna, Suchorzewski, Piszczyk, & Haponiuk, 2020), (Członka, Strąkowska, & Kairyte, 2020). This aligns with the information from Vestas' material passport, which indicates that WTB waste contains PUR adhesives.

3.2 Chemical Recycling

3.2.1 Low temperature and pressure Solvolysis

Figure 17 presents the TGA data, indicating that the best results were obtained in Experiment 13. This experiment involved using 200 grams of PEG200, 12.5 grams of NaOH, and 10 grams of GFRPs at 200°C over 5.5 hours, achieving a decomposition efficiency of about 80%.

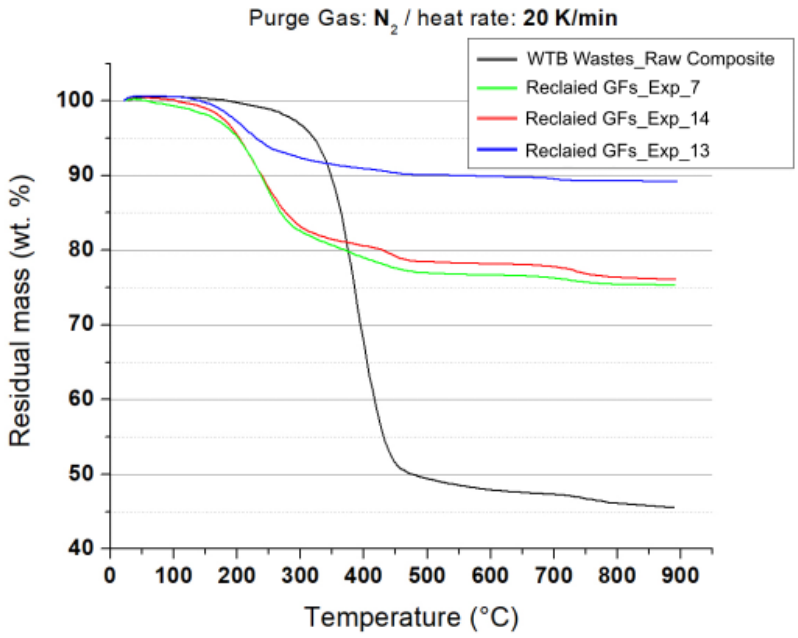

Figure 17: TGA Analysis of WTB Waste and Experiments 7, 13 and 14

In addition to the TGA results, the reclaimed fibres were examined using Scanning Electron Microscopy (SEM), with Energy Dispersive X-ray Spectroscopy (EDX) providing further visual confirmation. It is worth mentioning that while catalysts such as NaOH are effective in breaking down the matrix and recovering fibres, they also cause some degree of damage to the fibres during the process (Bashir, Yang, & Liggat, 2018).

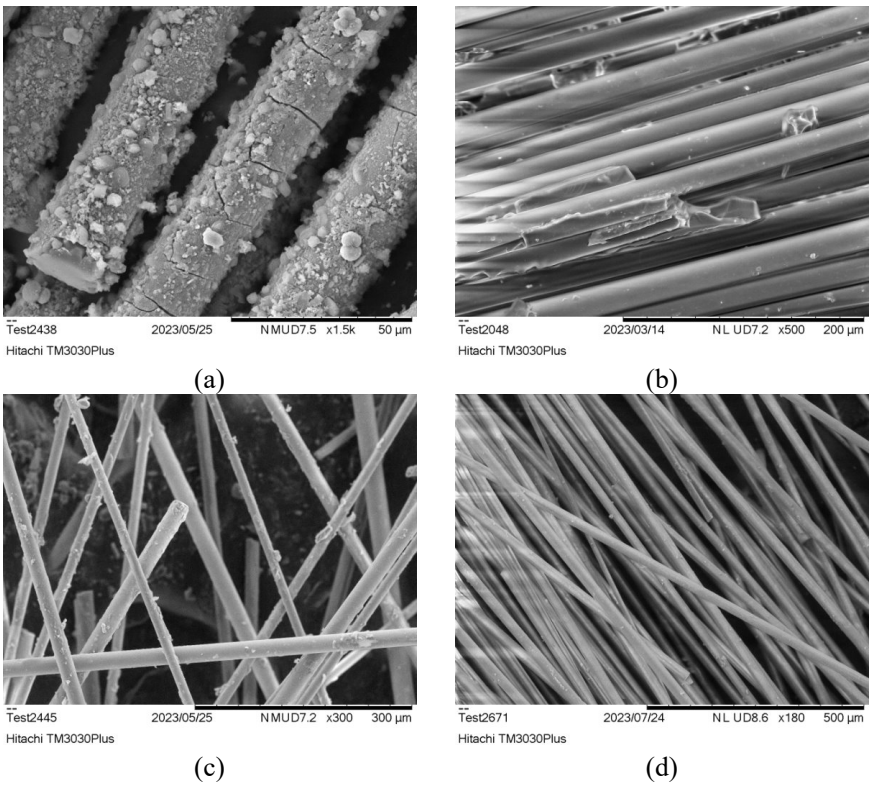

Figure 18:SEM images of Reclaimed Fibres from (a) Exp 12, (b) Exp 7, (c) Exp 14, (d) Exp 13.

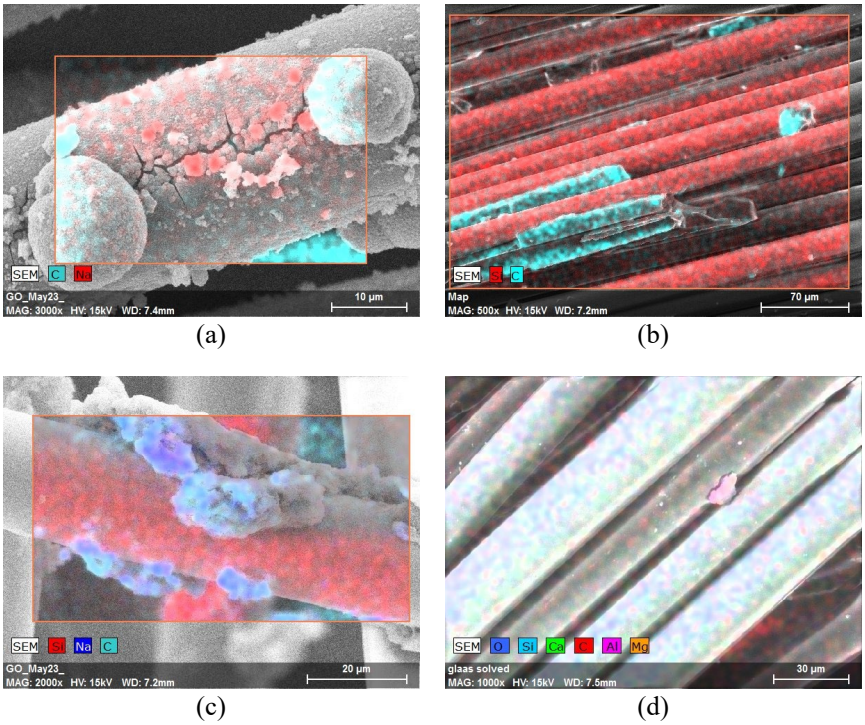

Figure 19:EDX Analysis of Reclaimed Fibres from (a) Exp 12, (b) Exp 7, (c) Exp 14, (d) Exp 13.

3.2.2 Solvolysis at near- or supercritical conditions

The TGA analysis indicated that the optimal conditions, resulting in the shortest reaction time with a 100% yield, were achieved in Experiment 11.

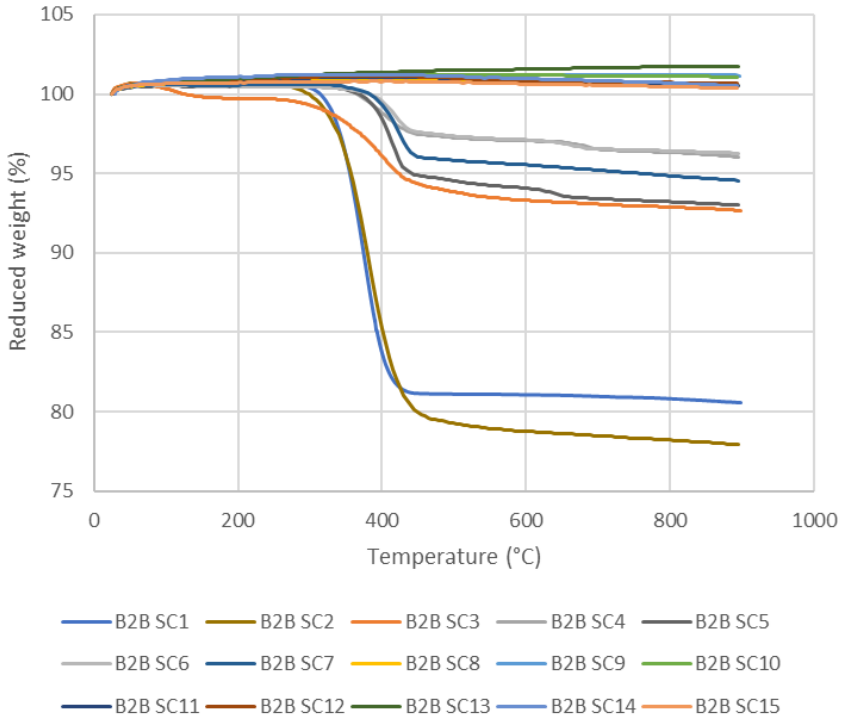

Figure 20: TGA Analysis of rGFs from Supercritical Acetone.

Additionally, SEM analysis was conducted on the recovered fibres, providing a visual representation of the results obtained from the TGA analysis. The use of these techniques confirmed that supercritical acetone effectively degrades the polymer matrix and recovers the fibres without causing any damage to the fibre structure.

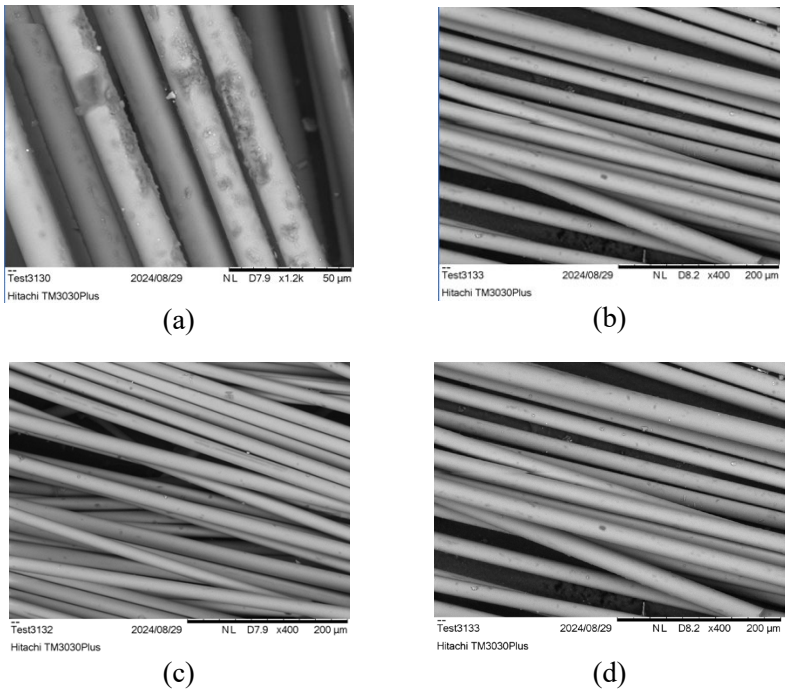

Figure 21: SEM images of Reclaimed Fibres from (a) Exp 5, (b) Exp 7, (c) Exp 11, (d) Exp 14.

3.3 Thermal Recycling

3.3.1 Thermogravimetric analysis (TGA)

Although a simple optical inspection revealed that the raw waste primarily consisted of glass fibre-reinforced polymer (GFRP), it was evident that the material was an inhomogeneous mixture, including chunks of other materials, such as wood. To account for this variability, a series of TGA measurements were conducted. Due to limitations of the sample holder, the analyses were performed on samples from the smallest particle size fraction (i.e., less than 0.063 mm). Figure 22 shows the TGA results for three different samples under an inert nitrogen atmosphere. Interestingly, the measurements showed only minor differences among the samples, despite the inherent inhomogeneity of the raw material. In all cases, the primary weight loss occurred in a single stage between 300–500°C, corresponding to the decomposition of the matrix polymer. By 700°C, the total weight loss stabilized at approximately 60%. Despite the variability in the composition of the GFRP waste, its thermal degradation behaviour remains relatively consistent.

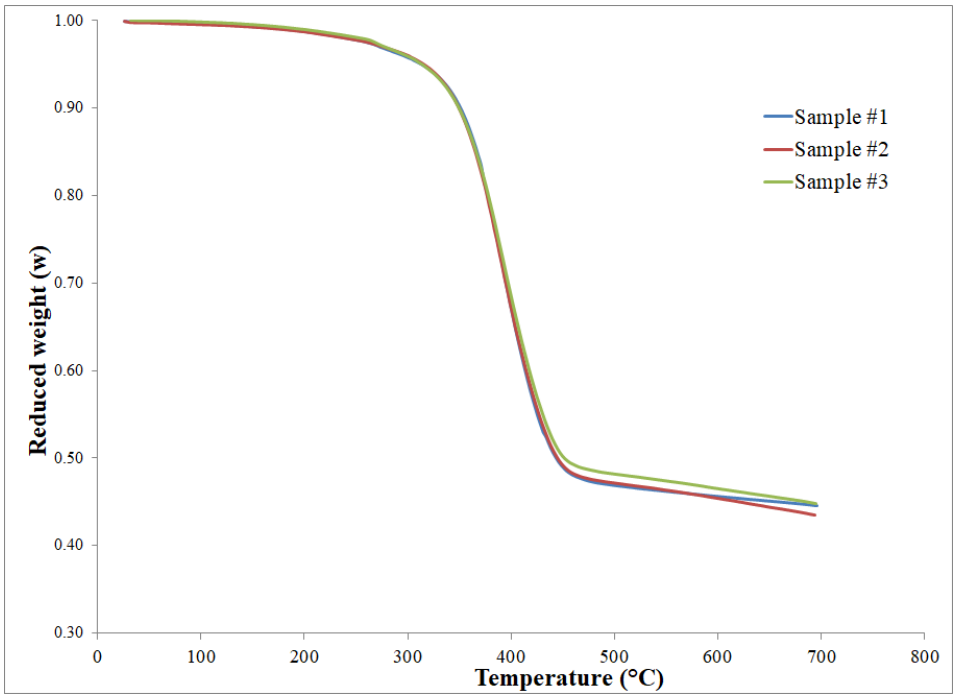

Figure 22: TGA measurements of GFRP WTB waste in inert atmosphere (N2, scan rate 20 K/min).

To further understand the effect of atmospheric conditions on the decomposition of GFRP waste, additional TGA measurements were performed under both inert (nitrogen) and air atmospheres. Figure 23 compares the results, demonstrating that the presence of oxygen significantly influences the decomposition process.

Specifically, the weight loss in air atmosphere was observed to be higher, reaching approximately 70% at 600°C, compared to the inert atmosphere. Additionally, the decomposition mechanism in the

presence of oxygen appeared to be more complex, likely due to oxidative reactions that occur alongside the thermal degradation of the polymer matrix.

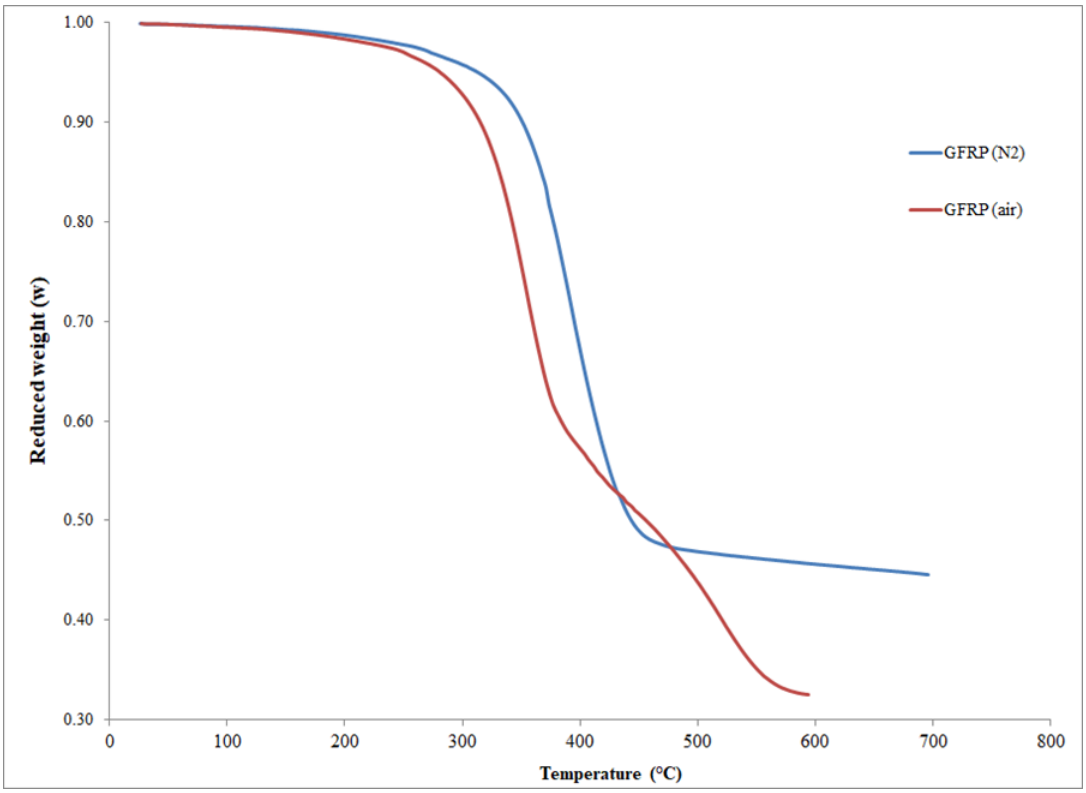

Figure 23: Comparative TGA measurements of GFRP WTB waste in inert and air atmosphere (scan rate 20 K/min).

Figure 24 shows the comparative weight loss rates of GFRP waste under inert and oxidative atmospheres, derived from the TGA measurements. In the inert atmosphere, a single decomposition event was observed, with the maximum rate occurring at approximately 400°C. In contrast, under an oxidative atmosphere, two overlapping weight loss peaks were evident within the temperature range of 250–600°C.

The first stage of weight loss, which aligns with the decomposition observed under inert conditions, can be attributed to the degradation of the GFRP matrix. Due to the presence of oxygen, this peak shifted to a lower temperature, with the maximum rate occurring around 370°C. The second stage, unique to the oxidative atmosphere, corresponds to the oxidation of the carbonaceous residual, with the maximum oxidation rate occurring at approximately 520°C. The respective weight loss percentages for these stages were approximately 45% and 20%. The presence of oxygen introduces

additional oxidation reactions, resulting in a more complex weight loss pattern compared to the single-stage decomposition observed under inert conditions.

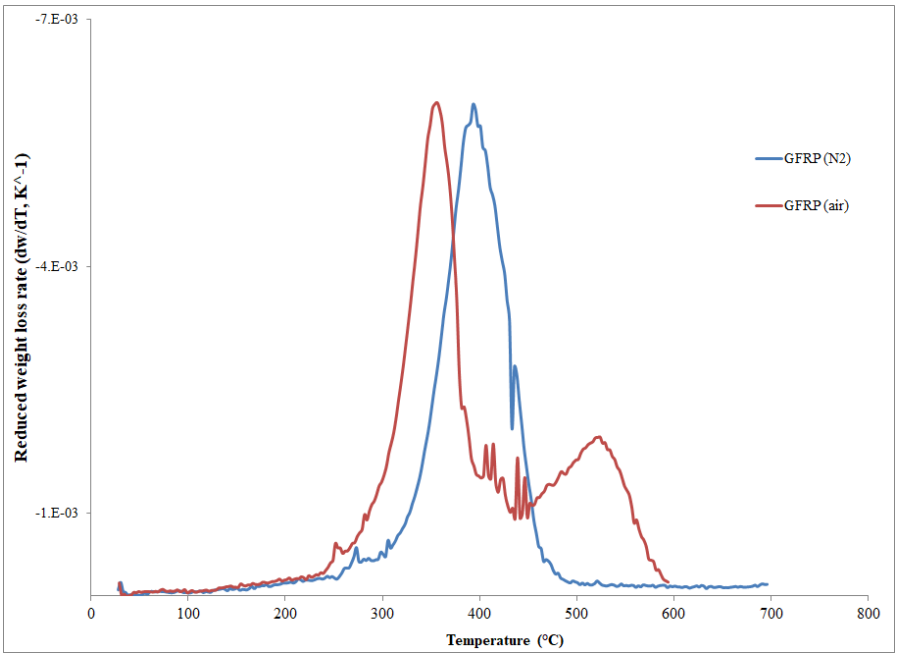

Figure 24: Comparative weight loss rates (calculated from the TGA measurements) of GFRP WTB waste in inert and air atmosphere (scan rate 20 K/min).

3.3.2 Sieving of the thermolyzed waste

The distribution of particle sizes in the thermolysis product was investigated through sieving. An initial test was conducted using the product from Run #13, where the initial waste feed had a particle size of 1–2 mm. The product was separated into four different size fractions, as shown in Figure 25. The results revealed that the majority of the product, approximately 80%, consisted of particles with a size larger than 1.0 mm, while around 15% of the material had a particle size smaller than 0.25 mm.

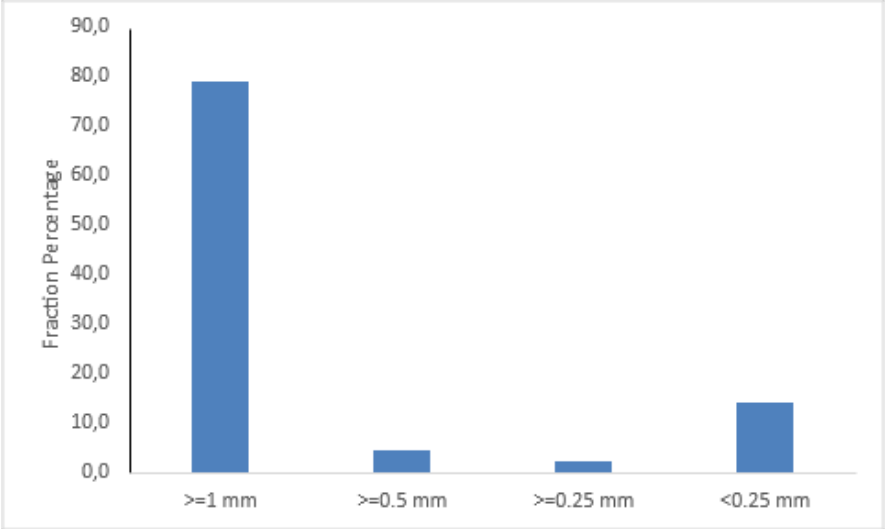

Figure 25: Particle size distribution of thermolyzed product from Run #13.

A more detailed investigation of particle size distribution was conducted using the product from Run #33. The initial batch consisted of 180.0 g of GFRP waste, which, after pyrolysis, produced a residual mass of 110.7 g, corresponding to a pyrolysis yield of 0.615. The GFRP waste used for thermolysis had an initial size distribution of 1–2 mm and was processed without further size adjustments.

From the pyrolysis product, a 50 g sample was carefully selected to ensure it was representative of the entire batch, while the remaining 60.7 g was subjected to sintering. The sintered product had a final mass of 52.0 g, yielding a sintering efficiency of 0.857. The pyrolyzed material was then sieved using a set of 4 sieves with mesh sizes of 1 mm, 500 μm, 250 μm, and 125 μm, separating the product into 5 distinct fractions.

The particle size distribution of the pyrolyzed GFRP waste, shown in Figure 26, revealed that approximately 90% of the material had a size above 0.50 mm, with about two-thirds exceeding 1 mm. This particle size distribution is attributed to the nature of the pyrolysis product, where the particles were partially fused due to the presence of tarry byproducts. These byproducts, which were not fully removed during pyrolysis, acted as a binding agent between the elongated particles derived from the chopped GFRP.

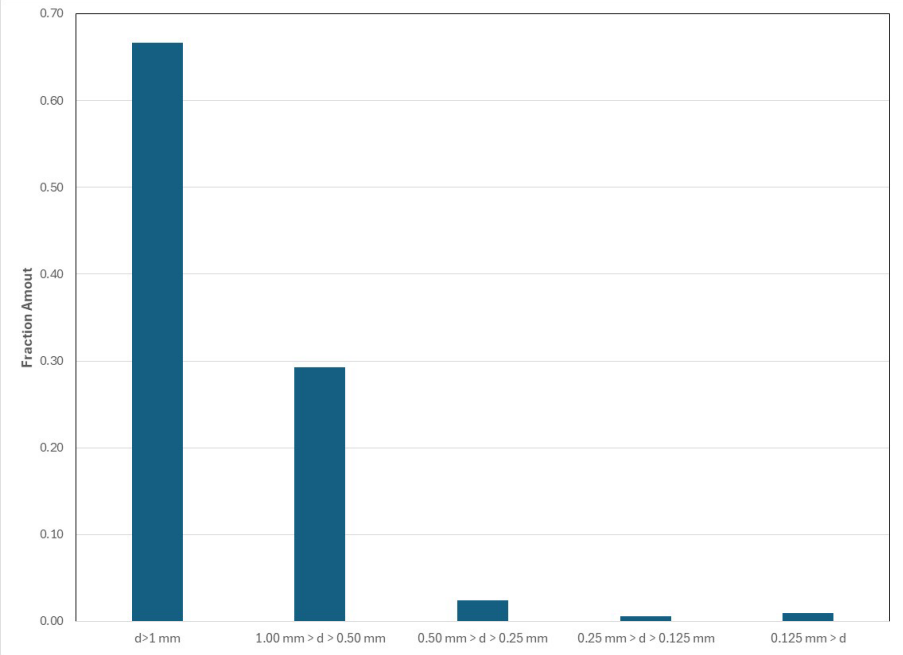

Figure 26: Particle size distribution of pyrolyzed product from Run #33.

Sieving of the final thermolyzed product enabled the separation into two distinct fractions: one consisting almost exclusively of glass fibres and the other comprising inorganic particles. Figure 27 the particle size distribution for the overall thermolyzed material, as well as for each of the two fractions.

Approximately 45% of the glass fibre fraction had a particle size below 1 mm, with around 15% smaller than 0.125 mm. When compared to the 1–2 mm nominal size of the initial waste, this significant reduction in size indicates that the chopping process caused considerable damage to the GFRP material. The inorganic particle fraction, however, displayed high inhomogeneity, with different types of particles distributed across various size ranges.

The fraction with particle sizes above 0.500 mm contained small rocks or pebbles and oxidized metal particles, which could be identified by their reddish colour. In contrast, the fraction below 0.125 mm was composed of a greyish powder, likely originating from the inorganic components of a paint

coating. The presence of such undesirable materials, particularly in the larger particle size fractions, suggests that these fractions are not suitable for inclusion in the final recycled product.

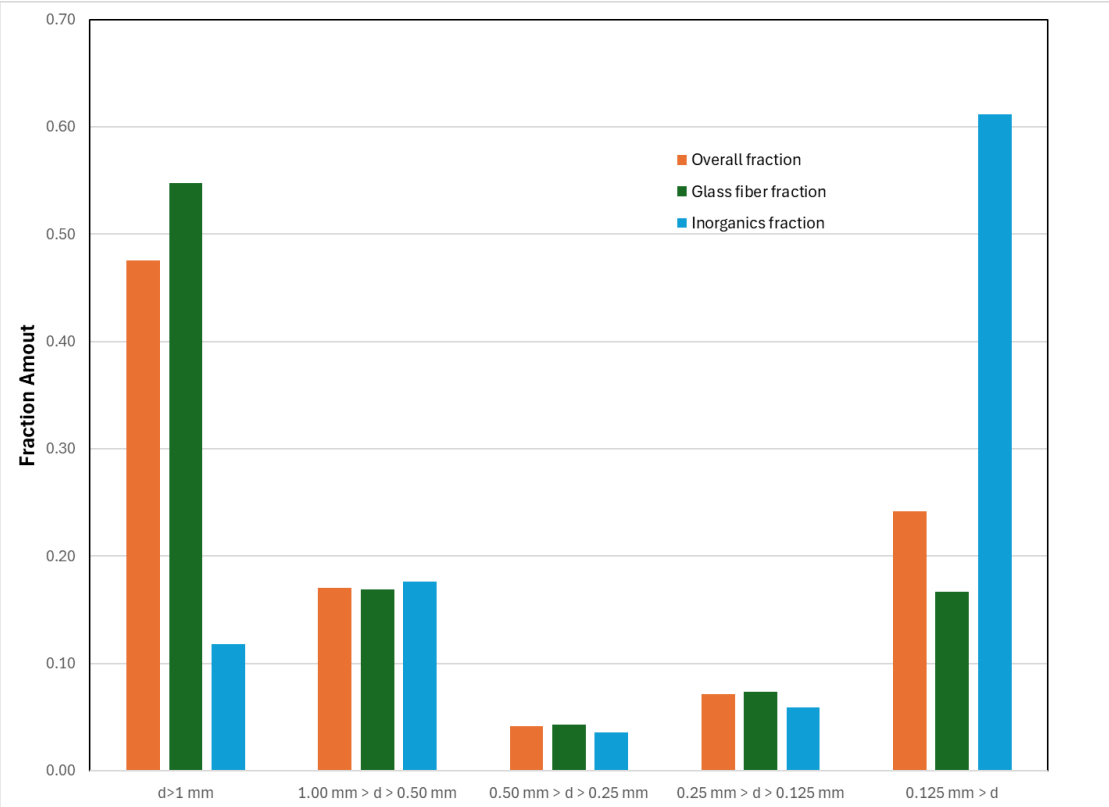

Figure 27: Particle size distribution of thermolyzed product, the glass fibre fraction and the inorganics fraction from Run #33.

3.4 Mechanical Recycling

Figure 28 shows the mean diameter of mortar flow for different mortar samples incorporating WTBF, with and without the addition of SP. The reference sample (Ref) exhibited a mean flow diameter of 13.38 cm in the absence of SP, which significantly increased to 18 cm (an increase of 34.5%) upon SP addition. This trend was consistent across all WTBF-reinforced samples. Specifically, the W0.5 sample showed an increase in flow diameter from 12.6 cm to 17.33 cm (an increase of 37.5%), the W1 sample from 11.8 cm to 15.93 cm (an increase of 35%), and the W2 sample from 11 cm to 14.58 cm (an increase of 32.5%) when SP was added.

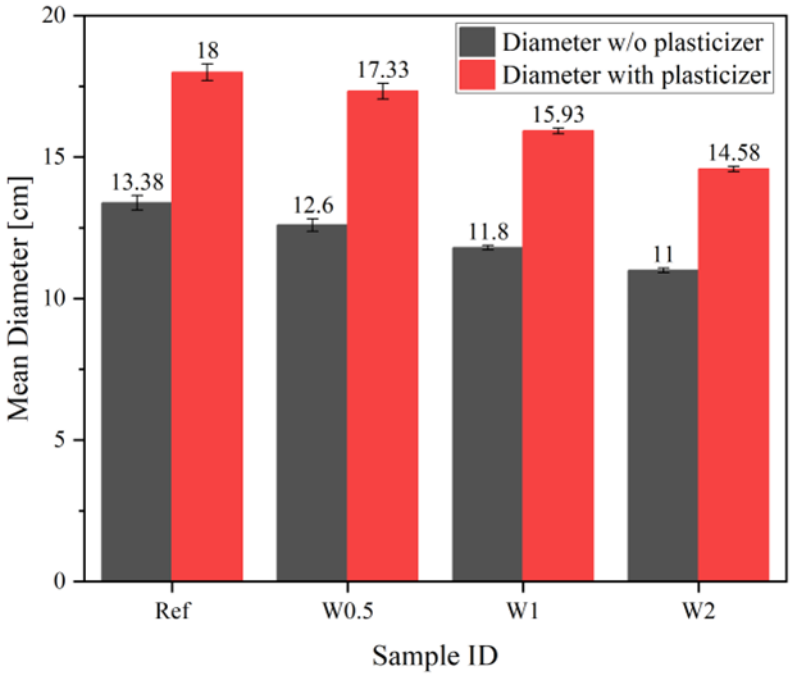

Figure 28: Flow of WTBF reinforced mortar with and without SP.

The reference sample (Ref) showed a compressive strength of 46.9 MPa without SP, which increased to 65.2 MPa with SP, resulting in a 39% increase. For the W0.5 sample, the compressive strength increased from 41.3 MPa to 65.1 MPa, marking a 58% increase. The W1 sample exhibited a notable improvement, with its compressive strength rising from 37.9 MPa to 63.5 MPa, reflecting a 68% increase. The most substantial enhancement was observed in the W2 sample, which saw its compressive strength jump from 28.2 MPa to 56.6 MPa, representing a remarkable 101% increase. Figure 29 (a) provides a concise comparison of the Compressive strengths at 28 days for different samples, showing the impact of both including and excluding SP and their corresponding strength gains. These results emphasize the significant enhancement in compressive strength achieved by incorporating SP.

Figure 29 (b) illustrates the results of flexural strength, comparing samples with and without SP at 28 days. The flexural strengths increased by approximately 24% for Ref (from 6.7 to 8.3), 19% for W0.5 (from 6.7 to 8), 30% for W1 (from 6.9 to 9), and 31% for W2 (from 5.9 to 7.7) when SP was added. Figure 29 (b) provides a concise comparison of the flexural strengths at 28 days for different samples, showing the impact of both including and excluding SP and their corresponding strength

gains. The results clearly demonstrate that samples incorporating SP consistently exhibited higher flexural strengths compared to those without, showing strength gains ranging from 19% to 31%.

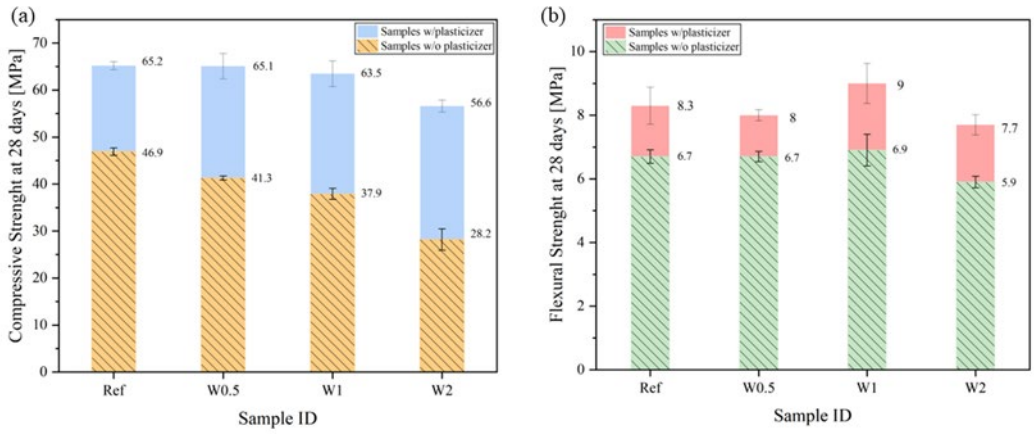

Figure 29: Mortars with and without SP at 28 days (a) Compressive strength; (b) Flexural strength.

4 CONCLUSIONS

4.1 Main conclusions

The research and development efforts under WP2 of the Blades2Build project successfully demonstrated the feasibility of various recycling methods for WTB waste, focusing on chemical, thermal, and mechanical recycling techniques. Each method exhibits distinct advantages and limitations, depending on the intended application and specific process requirements.

Thermal recycling was carried out through a batch thermolysis process consisting of two stages: pyrolysis in a nitrogen atmosphere and oxidation or sintering in an air atmosphere. The process duration was optimized, reducing the pyrolysis stage to approximately 90 minutes and the sintering stage to 30 minutes, while the batch size was scaled up to 300 g. Over the course of 33 runs, a total of 3.5 kg of thermolyzed product was produced, with an overall efficiency of 79%, representing the inorganic content of the WTB waste. Additionally, the separation of GFRP particles from the rest of the WTB waste (e.g., by flotation) was identified as a potential method to improve process efficiency. Sieving of the thermolyzed material proved to be an effective technique for removing undesirable inorganic admixtures, significantly enhancing the quality of the final product. Pyrolysis, while showing potential for scalability as a batch process, it also exhibits some disadvantages, due to the high temperatures required, typically between 500–600°C. It is also a time-intensive process, requiring up to 4–5 hours due to the need for an additional 1 to 1.5 hours for the system to reach the high temperatures for each step, with a continuous nitrogen flow required to maintain an inert atmosphere during the pyrolysis stage. Furthermore, post-pyrolysis treatment, involving oxidation in atmospheric conditions at temperatures between 400–500°C, adds to the energy demand and process complexity.

Chemical recycling was investigated through two main approaches: low-temperature and pressure solvolysis and solvolysis under supercritical conditions. Both methods face challenges in scalability due to their reliance on batch processing, extensive solvent and catalyst requirements, and the generation of significant liquid waste. However, the fibres recovered through chemical recycling are cleaner compared to those from pyrolysis, with processes operating at lower temperatures (200–350°C) and requiring shorter reaction times. Between the two methods, low-temperature solvolysis was found to cause fibre damage due to the use of NaOH as a catalyst, as confirmed by SEM and EDX analyses. This observation supports a shift toward discontinuing such catalysts in favor of more sustainable alternatives. In contrast, supercritical solvolysis with acetone demonstrated greater environmental sustainability, as acetone could be recovered and reused. However, the requirement for highly specialized and costly equipment for supercritical conditions limits its scalability, whereas low-temperature solvolysis operates with simpler setups.

Mechanical recycling was performed to shred the GFPR into small particles as fiber size. Afterwords, the wind turbine blade waste fiber was introduced into mortar as fiber reinforcement. The addition of WTBF slightly decreases the compressive strength and 1 vol. % of WTBF shows the highest flexural strength (6.91 MPa without SP, 8.95 MPa with SP) among samples regardless of SP additions. Furthermore, the positive correlation between increased flowability and strength suggests that improved workability leads to better compaction, resulting in stronger mortar strength. SP and fiber content show a synergistic effect on mortar properties. While higher fiber content improves the mechanical properties but reduces flowability, presenting a challenge in practical applications. SP effectively addresses this by significantly enhancing workability without compromising the mechanical performance provided by the fibers. The combination of SP and WTBF leads to an optimized balance between fresh and hardened properties, making it a promising solution for sustainable construction materials

This deliverable focused on achieving three main goals: maximizing material recovery, minimizing environmental impact, and ensuring industrial scalability. To maximize material recovery, optimized process conditions were identified, including reducing treatment durations, scaling up batch sizes, and exploring separation techniques such as flotation and sieving to enhance the quality of the recovered materials.

Minimizing environmental impact was addressed through chemical recycling, where process temperatures were significantly reduced compared to thermal methods, and treatment durations were optimized. Additionally, the project explored environmentally friendly alternatives such as switching to acetone as a recyclable solvent in supercritical solvolysis. Future stages of the project will include Life Cycle Assessment (LCA) to quantify the environmental impact of these processes and provide a more holistic evaluation.

To ensure industrial scalability, thermal and chemical recycling processes were scaled up to pilot units. Furthermore, mechanical recycling, due to its relatively straightforward implementation, is planned for industrial-scale deployment through a plant being developed by PreZero, showcasing its practical application in large-scale operations.

4.2 Action points

Moving forward, the focus will remain on supporting the material needs of the project partners by providing recycled glass fibres. Emphasis will be placed on maintaining the optimized recycling processes established during Task 2.2, ensuring consistency in fibre quality and scalability to meet the demands of the project partners.

4.3 Deviations from DoA

No deviations from DoA

5 BIBLIOGRAPHY

[1] C. Morin, A. Loppinet-Serani, F. Cansell and C. Aymonier, " Near- and supercritical solvolysis of carbon fibre reinforced polymers (CFRPs) for recycling carbon fibers as a valuable resource: State of the art," *J. Supercrit. Fluids,* vol. 66, pp. 232-240, 2012.

[2] G. Oliveux, J.-L. Bailleul and E. L. G. L. Salle, "Chemical recycling of glass fibre reinforced composites using subcritical water," *Compos. Part Appl. Sci. Manuf.,* vol. 43, no. 11, pp. 1809-1818, Nov 2012.

[3] C. Podara, S. Termine and M. Modestou, "Recent Trends of Recycling and Upcycling of Polymers and Composites: A Comprehensive Review," *Recycling,* vol. 9, no. 3, June 2024.

[4] E. Morici and N. Dintcheva, "Recycling of Thermoset Materials and Thermoset-Based Composites: Challenge and Opportunity.," *Polymers,* no. 14, p. 4153, 2022.

[5] W. Dang, M. Kubouchi, H. Sembokuya and K. Tsuda, "Chemical recycling of glass fiber reinforced epoxy resin cured with amine using nitric acid," *Polymer,* vol. 6, no. 46, pp. 1905-1912, February 2005.

[6] N. Koto and B. Soegijono, “Effect of Rice Husk Ash Filler of Resistance Against of High-Speed Projectile Impact on Polyester-Fiberglass Double Panel Composites.,” *Journal of Physics: Conference Series.,* p. 1191, 2019.

[7] M. Chukwu, C. Madueke and L. Ekebafe, “Effects of Snail Shell as Filler on the Mechanical Properties of Terephthalic Unsaturated Polyester Resin,” 2019.

[8] L. Z. S. S. Simitzis, DSC curing study of catalytically synthesized maleic-acid-based unsaturated polyesters, Polym. Inter., vol. 51, 2002, pp. 308-318.

[9] A. Gopanna, R. Mandapati and S. Thomas, “Fourier transform infrared spectroscopy (FTIR), Raman spectroscopy and wide-angle X-ray scattering (WAXS) of polypropylene (PP)/cyclic olefin copolymer (COC) blends for qualitative and quantitative analysis,” *Polym Bull,* vol. 79, pp. 4259-4274, 2019.

[10] H. R. Nafchi, M. Abdouss, S. K. Najafi, R. M. Gargari and M. Mazhar, “Effects of nano-clay particles and oxidized polypropylene polymers on improvement of the thermal properties of wood plastic composite,” *Maderas. Ciencia y tecnologia,* vol. 17, no. 1, pp. 45-54, 2015.

[11] A. Ul-Hamid, K. Al-Soufi, L. Al-Hadhrami and A. Shemsi, “Failure investigation of an underground low voltage XLPE insulated cable.,” *Anti-Corrosion Methods and Materials.,* vol. 62, pp. 281-287., 2015.

[12] M. Pandey, G. Joshi, A. Mukherjee and P. Thomas, “Electrical properties and thermal degradation of poly(vinyl chloride)/polyvinylidene fluoride/ZnO polymer nanocomposites.,” *Polymer International.,* 2016.

[13] I. Fernandes, R. Santos, E. Araujo dos Santos, T. Rocha, N. Domingues and C. A. Moraes, “Replacement of Commercial Silica by Rice Husk Ash in Epoxy Composites: A Comparative Analysis.,” *Materials Research,* 2018.

[14] Zhang and .. Liu, “Superhydrophobic Surface with Gamma Irradiation Resistance and Self-Cleaning Effect in Air and Oil.,” *Coatings,* 2020.

[15] V. Emmanuel, B. Odile and R. Céline, “FTIR spectroscopy of woods: A new approach to study the weathering of the carving face of a sculpture, Spectrochimica Acta Part A: Molecular and Biomolecular Spectroscopy,” *Spectrochimica Acta Part A: Molecular and Biomolecular Spectroscopy,* vol. 136, no. Part C, pp. 1255-1259, 2015.

[16] P. Kosmela, A. Hejna, J. Suchorzewski, Ł. Piszczyk and J. Haponiuk, “Study on the Structure-Property Dependences of Rigid PUR-PIR Foams Obtained from Marine Biomass-Based Biopolyol.,” *Materials,* 2020.

[17] S. Członka, A. Strąkowska and A. Kairyte, “Application of Walnut Shells-Derived Biopolyol in the Synthesis of Rigid Polyurethane Foams.,” *Materials,* vol. 13, 2020.

[18] S. Bashir, L. Yang and J. Liggat, “Kinetics of dissolution of glass fibre in hot alkaline solution,” *J Mater Sci,* vol. 58, p. 1710–1722, 2018.